RSC Advances

This is an *Accepted Manuscript*, which has been through the Royal Society of Chemistry peer review process and has been accepted for publication.

Accepted Manuscripts are published online shortly after acceptance, before technical editing, formatting and proof reading. Using this free service, authors can make their results available to the community, in citable form, before we publish the edited article. This *Accepted Manuscript* will be replaced by the edited, formatted and paginated article as soon as this is available.

You can find more information about *Accepted Manuscripts* in the Information for Authors.

Please note that technical editing may introduce minor changes to the text and/or graphics, which may alter content. The journal's standard Terms & Conditions and the Ethical guidelines still apply. In no event shall the Royal Society of Chemistry be held responsible for any errors or omissions in this *Accepted Manuscript* or any consequences arising from the use of any information it contains.

ROYAL SOCIETY OF CHEMISTRY

www.rsc.org/advances

Dynamic Article Links▶

Cite this: DOI: 10.1039/c0xx00000x

www.rsc.org/xxxxxx

COMMUNICATION

Ultraviolet photoconductivity of amorphous ZnAlSnO thin-film transistors

Q. J. Jiang,[a] C. J. Wu,[a] L. S. Feng,[a] G. Y. Yu,[a] L. Gong,[b] Z. Z. Ye,[a] J. G. Lu* [a]

Received (in XXX, XXX) XthXXXXXXXXX 20XX, Accepted Xth XXXXXXXXX 20XX
DOI: 10.1039/b000000x

Ultraviolet (UV) photoconductivity of solution-processed amorphous zinc-aluminum-tin oxide (*a*-ZATO) TFTs has been investigated in detail to clarify the device responses. The sensitivities of *a*-ZATO TFTs towards UV light are strongly dependent on the Al content. The UV exposure and recover process are decided by the state changes of oxygen defects (V_O^0 and V_O^{2+}). An appropriate Al addition can not only reduce the amounts of photogenerated carriers by increasing the band gap of ZATO films, but also markedly decrease the UV photoconductivity and recovery time, which benefits the TFT applications in the display fields. Based on UV behaviors of ZATO TFTs, a feasible and reasonable mechanism model has been proposed, which provides a fundamental sight of UV photoconductivity of ZATO TFTs and may also be applied to other AOS TFTs.

Recently, wide-band gap metal oxide semiconductors, especially for amorphous ones, have attracted great attention in fields of transparent displays, electronic and electro-optic components.[1-5] With high mobility, excellent optical transparency and long-term stability, amorphous oxide semiconductors (AOSs) are commonly used as thin-film transistor (TFT) channels to realize high pixels, high frame rate and high resolution displays.[6,7] Up to now, amorphous indium-gallium-zinc oxide (*a*-IGZO) and amorphous zinc-indium-tin oxide (*a*-ZITO) are the most attractive materials for practical applications.[8-10] The above focuses of AOSs are almost all on electro-optic and display devices. However, AOSs can also be used as effective phototransistors and photosensors, which is a very potential and promising research area.[10] Compared to the conventional photodiodes, AOS phototransistors exhibit much larger sensitivity, lower noise and better characters for integrated circuit, and these advantages deserve further investigation.[11,12]

In our previous reports, we have demonstrated indium-free amorphous zinc-aluminum-tin oxide (*a*-ZATO) TFTs with excellent electrical performances and long-term stability,[13] which are very promising for commercial applications in next-generation displays. In practical applications, most of their uses will be exposed to a backlight or ambient light during operation, ~~so the light sensitivity of ZATO TFTs is critically important. In~~ addition, for a wide range of functional applications such as future phototransistors, it is also very necessary to have a precise knowledge of the effect of light on device behaviors. In this letter, we conduct a study of ultraviolet (UV) photoconductivity in *a*-ZATO TFTs. The UV effects on performances of *a*-ZATO TFTs are investigated in detail. A mechanism model is proposed to reveal the photoconductivity and device stability during operation. This work provides a feasible model to explain UV behaviors of *a*-ZATO TFTs. More importantly, this model can also be used to other AOS TFTs for understanding the UV responses.

The ZATO precursors were prepared by a combustion solution process with mixing the single precursor.[13] The channel films were made on n^{++} Si/150 nm SiO_2 wafers (University Wafer) by spinning coating using a combustion solution process. 100 nm Al films prepared by electron beam evaporation were used as the source and drain electrodes. The TFT channel width and length were 1000 and 200 μm, respectively. Details could be found in our previous report.[13] Here, the Al content (in molar ratio) is 0, 0.5, 1.0 and 2.0, thus the samples are correspondingly designed as ZATO (0), ZATO (0.5), ZATO (1.0) and ZATO (2.0), respectively.

The electrical properties of the *a*-ZATO films were carried out on an HL5500 system using a four-point probe van der Pauw configuration. The optical transmission through film was performed with a UV 3600 ultraviolet-visible spectrophotometer from 225 to 800 nm. Device electrical performances were measured by a source-meter system (Agilent Technologies E5270B) under dark and UV (365 nm, 60mWcm^{-2}) conditions. During the measurement, ZATO TFT devices were exposed to UV illumination and the electrical performances were carried out under UV (30 s, 2 min, 5 min, 10 min and 20 min) and after removing UV (10 s, 100 s, 500 s, 1000 s, 5000 s and 10000 s).

Fig. 1 depicts the I_{DS}-V_{DS} (drain current-drain bias) characteristics curves of *a*-ZATO (1.0) TFT under dark and 365 nm UV illumination (20 min) at V_{GS}= 0 V (V_{GS} is the gate bias). In both cases, I_{DS} increases as V_{DS} is elevated. At V_{DS}= 20 V, I_{DS}= 3.68×10^{-10} A under dark, which increases to 5.39×10^{-7} A under UV illumination. Similar data are observed at V_{DS}= -20 V. The resistance of the ZATO film is $1.25\times10^{9}\Omega$ cm under dark, which increases to $6.42\times10^{5}\Omega$ cm after UV illumination. These results confirm that the UV light (365 nm) can effectively promote the photoconductivity behaviors of the *a*-ZATO channels. The obvious increment of I_{DS} indicates that *a*-ZATO films are sensitive to the UV light and can be used as the phototransistors.

Fig. 2 shows the typical output characteristics of the *a*-ZATO

[a] *State Key Laboratory of Silicon Materials,School of Materials Science and Engineering, Zhejiang University, Hangzhou 310027, China.*
E-mail:lujianguo@zju.edu.cn;
[b] *School of Physics and Electronic Science, Changsha University of Science and Technology, Changsha 410114, China*
† Electronic supplementary information (ESI) available. See DOI:XXX

RSC Advances Accepted Manuscript

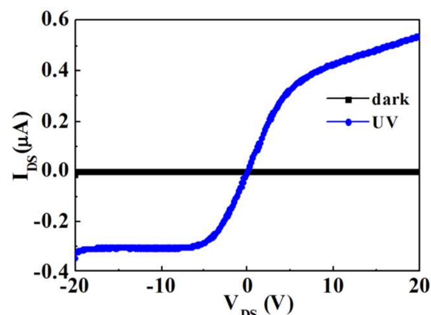

Fig. 1. I_{DS}-V_{DS} characteristic curves of *a*-ZATO (1.0) TFTunder dark and 365 nm UV illumination at V_{GS}= 0 V.

(1.0) TFT under dark, UV illumination (2 min) and recover periods (10 s, 1000 s) after UV illumination. Other related output curves are shown in Fig. S1 (ESI,†). For all the TFT devices, good ohmic contacts at the Al/channel interface have been formed due to no current crowding at low V_{DS}. A clear pinch-off and current saturation are observed. Moreover, the saturation current of I_{DS} markedly increases as the positive V_{GS} increases, indicating the devices operate in an enhanced mode with an *n*-type channel. Under dark condition, the *a*-ZATO (1.0) TFT exhibits a saturation current of 15.14 μA, while it increases to 47.88 μA after UV illumination for 2 min at V_{GS}=40 V. After removing the UV illumination, the saturation current decreases to 32.71 and 18.49 μA for recover durations of 10 and 1000 s, respectively. Therefore, it is believed that the photoelectric effect by UV contributes to the saturation current changes.

Here, *a*-ZATO TFTs with different Al contents (0, 0.5, 1.0 and 2.0) are used to investigate the UV photoconductivity.[14] Figs. 3(a), 3(c), 3(e) and 3(g) show the I_{DS}-V_{GS} curve changes of *a*-ZATO (0, 0.5, 1.0 and 2.0) TFTs under dark and UV illuminating (2 min and 20 min) at V_{DS} = 10 V. At off-state ($V_{GS}<V_{ON}$, V_{ON} is the open voltage), I_{DS} markedly increases more than 1–5 orders of magnitude under UV illumination as compared to that measured under dark, which is dependent on the Al content in the ZATO channels. Notably, the increased magnitude of I_{DS} under UV illumination gets much smaller as the Al content increases. This may be due to the enhanced optical energy band by Al addition, which makes the photogenerated carriers more difficult to produce. However, at on-state ($V_{GS}>V_{ON}$), UV exposure brings small changes of I_{DS}. In order to further study the recover changes after removing UV, various recover time (10 s, 100 s, 500 s, 1000s, 5000 s and 10000 s) are adopted to investigate the transfer characteristic. The corresponding recovering I_{DS}-V_{GS} curves are shown in Figs. 3(b), 3(d), 3(f) and 3(h). After removing the UV light (e.g., for 10 s), the off-current decreases quickly and the on-

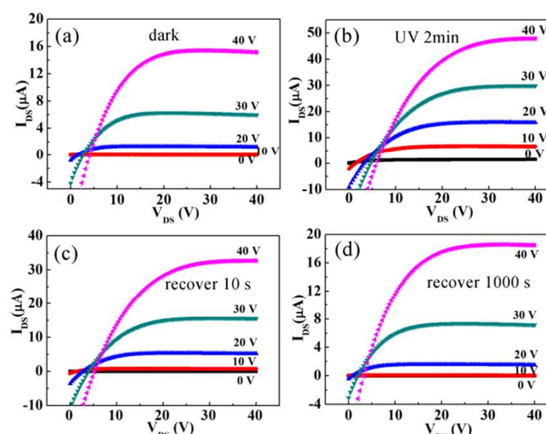

Fig. 2. Typical output characteristics of *a*-ZATO (1.0) TFT: (a) under dark, (b) under UV illumination for 2 min, (c) 10 s recover after UV exposure, and (d) 1000 s recover after UV exposure.

current slowly recovers to the original levels. With prolonging the recovering time, the device properties get slowly to recover back. After 10000 s, all the *a*-ZATO TFT devices recover to that of the dark conditions. Moreover, the recover speed gets quickly with Al content increasing. For ZATO (0) sample, the off-current recovers to the dark level of 10^{-10} A after 1000 s. With increasing Al content to 0.5, 1.0 and 2.0, the recovering time of the off-current to the dark conditions are decreased to 100 s. For these samples, with continuously increasing the recovering time (>1000 s), the off-current and on-current both show little variations, the V_{ON} shifts to be positive direction. Additionally, increasing Al addition results in the much quicker recovery of the V_{ON}.

Table 1 summarizes the changes of V_{th} and density of the interfacial trap states (N_t) at the ZATO channel/SiO_2 interface of *a*-ZATO TFTs under UV illumination and recovering periods. The V_{th} and N_t can be determined using the following equations:

$$I_{DS}^{1/2} = \sqrt{\frac{W}{2L} C_i \mu_{FE}} \left(V_{GS} - V_{th}\right) \qquad V_{DS} \geq V_{GS} - V_{th} \tag{1}$$

$$N_t = \left[\frac{SS \log(e)}{(kT/q)} - 1\right] \frac{C_i}{q} \tag{2}$$

where C_i, μ_{FE}, W, L, V_{th}, SS, e, K, T, and q are the capacitance per unit area of the gate insulator (0.023 μF/cm^2), field effect mobility, channel width, channel length, threshold voltage, subthreshold swing, Euler's constant, Boltzmann constant, temperature, and quantity of one electron, respectively.

The corresponding μ_{FE} and device response time ($\tau = R_{ON} \times C_i$) are shown in Table S1 and Table S2 (ESI,†). Here, we focus on the recover properties of the same TFT. As shown in Table 1, during the UV illumination, the V_{th} shifts to a very negative value

Table 1 V_{th} and N_t ($\times 10^{12}$ cm^{-2}) changes of *a*-ZATO (0, 0.5, 1.0 and 2.0) TFTs under UV illumination and the recovering period (dark, 10 s, 100 s, 500 s, 1000 s, 5000 s and 10000 s) after UV illumination.

	Samples	dark	UV 2min	10 s	100 s	500 s	1000 s	5000 s	10000 s
V_{th}	ZATO (0)	-0.13	-31.10	-21.14	-12.32	-3.82	-2.08	-0.56	-0.56
	ZATO (0.5)	5.32	-25.64	-5.90	-1.72	0.49	1.20	3.31	4.28
	ZATO (1.0)	12.19	-10.57	1.34	8.18	10.56	10.67	11.82	12.20
	ZATO (2.0)	6.66	-30.45	-3.75	3.17	5.22	6.17	6.43	6.54
N_t	ZATO (0)	1.48	40.67	28.77	14.69	3.78	2.00	1.09	1.08
	ZATO (0.5)	1.14	23.15	7.28	2.55	2.53	2.42	2.31	1.24
	ZATO (1.0)	0.77	16.13	9.62	2.66	1.88	1.29	1.04	0.97
	ZATO (2.0)	1.59	18.57	9.16	5.42	2.63	2.61	1.41	1.42

This journal is © The Royal Society of Chemistry [year]

RSC Advances Accepted Manuscript

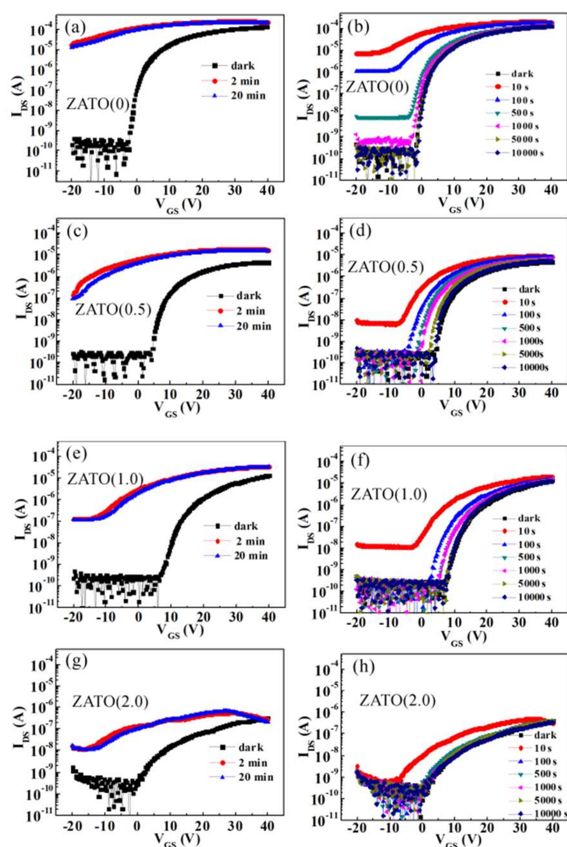

Fig. 3. I_{DS}-V_{DS} curves of *a*-ZATO TFTs at V_{DS} =10 V: (a) and (b) for ZATO (0), (c) and (d) for ZATO (0.5), (e) and (f) for ZATO (1.0), and (g) and (h) for ZATO (2.0) at UV illuminating and post recovering for different time (10, 100, 500, 1000, 5000, and 10000 s), respectively.

compared with that of the dark sample: from -0.13, 5.32, 12.19, and 6.66 V to -31.10, -25.64, -10.57, and -30.45 V for *a*-ZATO (0), *a*-ZATO (0.5), *a*-ZATO (1.0), and *a*-ZATO (2.0), respectively. However, after removing the UV sources, all TFTs exhibit a tendency that the V_{th} recovers to the dark value slowly with prolonging the recovering time. After 5000 s, the V_{th} values of all the samples recover to the original states except for small deviation. Additionally, the μ_{FE} and N_t values increase during the UV illumination, and then decrease slowly to the original states after removing the UV sources. While, for τ, the tendency is opposite compared with that of μ_{FE} changes. Therefore, we can see that an appropriate Al addition can do well for the TFT devices and UV detections.

Fig. S2 shows optical transmittance spectra of *a*-ZATO films with various Al contents. In general, the amorphous semiconductor is commonly a non-direct semiconductor. The optical band gap energies (E_g^{opt}) can be calculated by the Tuac relation,[15]

$$\alpha h\nu = C\left(h\nu - E_g^{opt}\right)^m \quad (3)$$

Where *h* is Planck's constant, *v* is the photon frequency, *α* is the absorption coefficient, and *C* is a constant. The value of *m* is 1/2 for a direct semiconductor and 2 for a non-direct semiconductor. The amorphous semiconductor is commonly a non-direct semiconductor. However, in order to determine the difference of band gap energies of an amorphous semiconductor, the *m* value induced by the direct semiconductor model has been usually used. Thus, we apply *m*=1/2 for our calculation.[15] The E_g^{opt} values are displayed in the inset of Fig. S2, which increase from 3.04 to 3.59 eV as the Al content increases from 0 to 2.0. The larger optical band gaps can not only enhance the barrier of the electron transition, thus decreasing the carrier concentration,[13] but also affect the UV photoconductivity of *a*-ZATO TFTs.

Based on the V_{th}, N_t, μ_{FE} and τ changes during the UV illumination and UV recover periods, we have proposed a mechanism model to illustrate the UV behaviors of *a*-ZATO TFTs. As Fig. 3 depicts, I_{DS} markedly increases upon UV illumination during the off-state. Moreover, with increasing V_{GS} from -20 V to the V_{ON}, I_{DS} continue increasing. As shown in Fig. 4 (a), in this process, electrons are mostly emitted into conduction band (E_c) from the valence band (E_v) by absorbing the UV photo energy (3.40 eV), which is larger than the band gap of ZATO films when $x\leq0.5$ (3.04 eV for ZATO (0) and 3.23 eV for ZATO (0.5)). While $x\geq1.0$, this direct electron transition will not occur due to the band gap is larger than UV energy (3.48 eV for ZATO (1.0) and 3.59 eV for ZATO (2.0)). Moreover, previous studies confirm neutral oxygen vacancies (V_O^0) always exist with a high density at the top of E_v to form deep levels.[16,17] The V_O^0 can be photo-excited to release two electrons to E_c by $V_O^0 \rightarrow V_O^+ + e$ and $V_O^+ \rightarrow V_O^{2+} + e$.[16] Therefore, for $x\leq0.5$, UV generated electrons in the band gap and V_O^0 contribute to the large I_{DS}. However, the electron transfer from E_v to E_c is the dominated reason for promoting photoconductivity in this case. For $x\geq1.0$, the photo-excited V_O^0 electrons dominate the I_{DS} enhancement, which makes the photoconductivity promoted. Moreover, we deduce these different reasons lead to the divergence of the I_{DS}–V_{GS} curves at off-state between the samples of $x\leq0.5$ and $x\geq1.0$. The persistent increment of I_{DS} with increasing V_{GS} at off-state is due to the electron accumulation at E_c. At off-state, the electrons tend to escape from the TFT electron transfer channel (close to the channel/SiO_2 interface) to the ZATO matrix, thus increasing the electrical properties of ZATO films and making the TFTs lose the transfer characteristics.[18] However, at on-state ($V_{GS}>V_{ON}$), small changes of I_{DS} occur due to that the gate-bias-induced charge carriers dominate the photo-induced carriers, as shown in Fig. 4(b). The divergence of I_{DS} values between the dark and UV conditions at on-state are resulted from the UV generated accumulation. Moreover, the intrinsic shallow centers between E_f and Ec can also act as electron trapping centers at on-state.[8] At on-state, all the electrons are accumulated close the channel/SiO_2 interface to form the electron transfer channel, which realizes the various electrical responses.[18]

After removing the UV sources, a persistent photoconductivity is observed, as shown in Fig. 4(c). Previous studies confirm that the excited O vacancies lead to the persistent photoconductivity in direct semiconductor. However, in AOS systems, the carrier recombination is much complex than crystalline semiconductor oxides due to the non-direct characters. For *a*-ZATO TFTs, we deduce four factors contribute to the carrier recombination:

1. Direct recombination of electrons at E_c and holes at E_v. Due to the non-direct character for *a*-ZATO AOSs, the direct recombination of electrons and holes needs the participation of lattice vibration. Moreover, Al addition can enlarge the band gap, which further shortens the recombination time. This is the reason for quicker recover of transfer characteristics with Al increasing, as shown in Figs. 3(b), 3(d), 3(f) and 3(h). Additionally, Al addition can decrease the *V*o in some extent, which will affect the lattice vibration. V_O^0 can form the ionized V_O^{2+} by capturing the photo-excited holes through $V_O^0 + 2h \rightarrow V_O^{2+}$, which will reduce the

RSC Advances Accepted Manuscript

direct recombination. These V_O^{2+} can exist stably in the ZATO

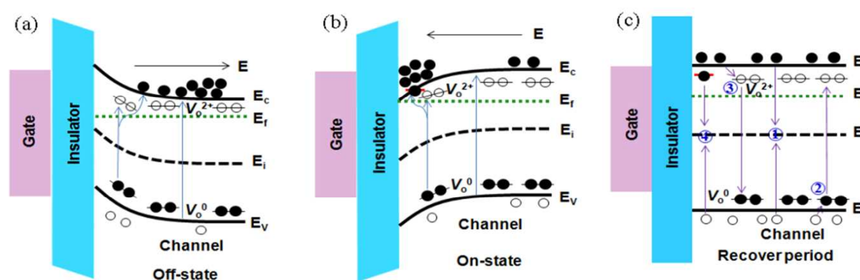

Fig. 4. Schematic diagram of mechanism model to illustrate the UV photoconductivity of *a*-ZATO TFTs.

films. In the recovery, the photo-excited holes of high-content Al samples ($x \geq 1.0$) are less than that of small content Al samples ($x \leq 0.5$). Therefore, less time is needed to recombine hole during the recovery for high Al content.

2. Some photo-excited V_O^{2+} during the UV illumination can return to the ground state (V_O^0) by thermal activation or other energy.[19-22] The existence of V_O^{2+} in the matrix can also combine the photo-excited electrons to form the ground state (V_O^0). The amounts of V_O^{2+} and photo-excited electrons result in the difference for various *a*-ZATO TFT recovery.

3. In AOS, there always exist some shallow levels to trap the electrons close to the ZATO/SiO_2 interface.[23, 24] During the recovery, the trapped electrons need long time to return to low energy level by relaxation. Thus, some trapped electrons are easily combined with the photo-excited holes to complete the recombination.

In summary, *a*-ZATO TFTs have been fabricated using a solution process for the UV investigation. The UV photoconductivity of *a*-ZATO TFTs have been investigated in detail. Results indicate that the sensitivities of *a*-ZATO TFTs towards to UV light are determined by the Al content. The Al content and O vacancies including V_O^0 and V_O^{2+} play a crucial role in the UV illumination and the recover process. An appropriate Al addition can markedly decrease the UV photoconductivity and recovery time, which is very beneficial for the TFT applications in the display fields. Moreover, the short recovery time is also a positive sign in UV detection with fast response. A feasible and reasonable mechanism model has been proposed to illustrate the TFT UV behaviors. This proposed model can give a fundamental sight of UV photoconductivity of AOS TFTs.

This work was supported by National Natural Science Foundation of China under Grant Nos. 51372002 and 51302021.

Notes and references

1 K. Nomura, H. Ohta, A. Takagi, T. Kamiya, M. Hirano, and H. Hosono, *Nature*, 2004,**432**, 488.

2 T. Kamiya, K. Nomura, and H. Hosono, *Sci. Technol. Adv. Mat.*, 2010,**11**, 044305.

3 C. J. Wu, X. F. Li, J. G. Lu, Z. Z. Ye, J. Zhang, T. T. Zhou, R. J. Sun, L. X. Chen, B. Lu, and X. H Pan, *Appl. Phys. Lett.*, 2013,**103**, 082109.

4 J. Zhang, X. F. Li, J. G. Lu, N. J. Zhou, P. J. Guo, B. Lu, X. H. Pan, L. X. Chen, and Z. Z. Ye, *RSC Adv.,* 2014,**4**, 3145.

5 Y. P. Wang, J. G. Lu, X. Bei, Z. Z. Ye, X. Li, D. Song, X. Y. Zhao, and W. Y. Ye, *Appl. Surf. Sci.*, 2011,**257**, 5966.

6 T. H. Hwang, I. S. Yang, O. K. Kwon, M. K. Ryu, C. W. Byun, C. S. Hwang, and S. H. Ko Park, *Jpn. J. Appl. Phys.*, 2011,**50**, 03CB06.

7 Q. J. Jiang, J. G. Lu, J. P. Cheng, X. F. Li, R. J. Sun, L. S. Feng, W. Dai, W. C. Yan, and Z. Z. Ye, *Appl. Phys. Lett.,* 2014,**105**, 132105.

8 J. Zhang, X. F. Li, J. G. Lu, Z. Z. Ye, L. Gong, P. Wu, J. Huang, Y. Z. Zhang, L. X. Chen, and B. H. Zhao, *J. Appl. Phys.,* 2011,**110**, 084509.

9 G. S. Heo, Y. Matsumoto, I. G. Gim, H. K. Lee, J. W. Park, and T. W. Kim, *Solid State Commun.,* 2010,**150**, 223.

10 T. H. Chang, C. J. Chiu, W. Y. Weng, S. J. Chang, T. Y. Tsai, and Z. D. Huang, *Appl. Phys. Lett.*, 2012,**101**, 261112.

11 Y. H. Kim, J. S. Heo, T. H. Kim, S. Park, M. H. Yoon, J. Kim, M. S. Oh, G. R. Yi, Y. Y. Noh, and S. K. Park, *Nature*, 2012, **489**, 128.

12 K. H. Lee, J. S. Jung, K. S. Son, J. S. Park, T. S. Kim, R. Choi, J. K. Jeong, J. Y. Kwon, B. Koo, and S. Y. Lee, *Appl. Phys. Lett.,*2009, **95**, 232106.

13 Q. J. Jiang, L. S. Feng, C. J. Wu, R. J. Sun, X. F. Li, B. Lu, Z. Z. Ye and J. G. Lu, *Appl. Phys. Lett.,* 2015,**106**, 053503.

14 K. Ghaffarzadeh, A. Nathan, J. Robertson, S. Kim, S. Jeon, C. Kim, U. I. Chung, and J. H. Lee, *Appl. Phys. Lett.,* 2010,**97**, 113504.

15 K. H. Lim, K. Kim, S. Kim, S. Y. Park, H. Kim, and Y. S. Kim, *Adv. Mater.,* 2013,**25**, 2994.

16 S. Lany and A. Zunger, *Phys. Rev. Lett.,* 2007,**98**, 045501.

17 P. Wu, J. Zhang, J. G. Lu, X. F. Li, C. J. Wu, R. J. Sun, L. S. Feng, Q. J. Jiang, B. Lu, X. H. Pan, and Z. Z. Ye, *IEEE Trans. Electron. Dev.*, 2014, **61**, 1431.

18 J. K. Jeong, H. W. Yang, J. H. Jeong, Y. G. Mo and H. D. Kim, *Appl. Phys. Lett.,* 2008,**93**, 123508.

19 S. Lany and A. Zunger, *Phys. Rev. B,* 2005,**72**, 035215.

20 A. Janotti, and C. G. Van de Walle, *Appl. Phys. Lett.,* 2005, **87**, 122102.

21 A. Janotti, and C. G. Van de Walle, *Phys. Rev. B,* 2007, **76**, 165202.

22 Y. Wang, Z. L. Liao, G. W. She, L. X. Mu, D. M. Chen, and W. S. Shi, *Appl. Phys. Lett.,* 2011,**98**, 203108.

23 J. M. Lee, I. T. Cho, J. H. Lee, and H. I. Kwon, *Appl. Phys. Lett.,* 2008,**93**, 093504.

24 K. Nomura, T. Kamiya, M. Hirano, and H. Hosono, *Appl. Phys. Lett.,*2009, **95**, 013502.

RSC Advances Accepted Manuscript

This journal is © The Royal Society of Chemistry [year]